Article

Not peer-reviewed version

A Miniature Multi-Functional Photoacoustic Probe

Riqiang Lin , Jiaming Zhang , Wen Gao , Xiatian Wang , Shengmiao Lv , Kwok-ho Lam * , Xiaojing Gong *

Posted Date: 10 May 2023

doi: 10.20944/preprints202305.0690.v1

Keywords: Miniature probe; Transparent ultrasound transducer; GRIN lens backing; OR-PAM.

Article

A Miniature Multi-Functional Photoacoustic Probe

Riqiang Lin [1,2], Jiaming Zhang [1], Wen Gao [2], Xiatian Wang [2], Shengmiao Lv [2], Kwok-ho Lam [1,3,*] and Xiaojing Gong [2,*]

[1] Department of Electrical Engineering, The Hong Kong Polytechnic University, Hung Hom, Kowloon, Hong Kong, China

[2] Research Center for Biomedical Optics and Molecular Imaging, Shenzhen Key Laboratory for Molecular Imaging, Guangdong Provincial Key Laboratory of Biomedical Optical Imaging Technology, CAS Key Laboratory of Health Informatics, Shenzhen Institute of Advanced Technology, Chinese Academy of Sciences, Shenzhen, 518055, China

[3] Centre for Medical and Industrial Ultrasonics, James Watt School of Engineering, University of Glasgow, Glasgow, Scotland, U.K.

* Correspondence: kwokho.lam@glasgow.ac.uk (K.-h.L.); xj.gong@siat.ac.cn (X.G.)

Abstract: Photoacoustic technology is a promising tool to provide morphological and functional information in biomedical research. To enhance the imaging efficiency, the reported photoacoustic probes have been designed coaxially involving complicated optical/acoustic prisms to bypass the opaque piezoelectric layer of ultrasound transducers, but leading to bulky probes and hindering the applications in limited space. Though the emergence of transparent piezoelectric materials helps to save the effort on the coaxial design, the reported transparent ultrasound transducers were still bulky. In this work, a miniature photoacoustic probe with an outer diameter of 4 mm was developed, in which an acoustic stack was made of the combination of transparent piezoelectric material and gradient-index lens as a backing layer. The transparent ultrasound transducer exhibited a high center frequency of ~47 MHz and a -6 dB bandwidth of 29.4%, which could be easily assembled with a pigtailed ferrule of a single-mode fiber. The multi-functional capability of the probe was successfully validated through the experiments of fluid flow sensing and photoacoustic imaging.

Keywords: miniature probe; transparent ultrasound transducer; GRIN lens backing; OR-PAM

1. Introduction

Photoacoustic technology, as a hybrid biomedical imaging modality [1,2], is capable of providing morphologic and functional information from cells to organs [3,4]. To ensure efficient irradiation and detection, the strategy of developing a coaxial construction of optical-acoustic beams and beam focusing is the warranted measure for probe design [5], such as optical-resolution photoacoustic microscopy (OR-PAM) [6–8]. As an essential element of system, lead zirconate titanate (PZT) has been used in ultrasound transducers for OR-PAM, which could hinder the laser delivering by its opaque appearance. To improve the system performance, the conventional OR-PAM essentially involves specific optical and acoustic designs [7,9], offering the coaxial excitation and detection to overcome the opaque issue of transducer. However, the transducer design with optical-acoustic prisms [7] is complicated and difficult to fabricate, making the imaging probe bulky and heavy.

To combine the ultrasound and optical beams coaxially, some transparent ultrasound transducers (TUTs) have been developed in recent years [10–14], providing solutions with flexibility on the PAM including the quadruple system [15]. Though lithium niobate (LN), one type of transparent piezoelectric single crystals, was commonly selected to develop the TUT in literature [10,11,14], there are still some challenges in the development of photoacoustic probes. First of all, the dimensions of most reported probes were ~1 cm. The LN wafer should be connected with electrical wires using conductive glue that adversely affects the transparency of the TUT. As for high-frequency transducers, the smaller aperture of the wafer would allow less room for electrical connection,

Preprints (www.preprints.org) | NOT PEER-REVIEWED | Posted: 10 May 2023 doi:10.20944/preprints202305.0690.v1

making the fabrication much more challenging. Secondly, indium tin oxide (ITO) is usually coated on the LN wafer as transparent electrodes of TUTs. In general, the thinner ITO coating offers better transparency but higher electrical resistance, causing an inefficient operation of the TUT. Thirdly, optical lenses used for focusing laser in the reported work were separated with the TUT such that a mount must be applied to fix and adjust the lens coaxially with the TUT. Therefore, the TUT with the lens mount would give a bulky photoacoustic probe, restricting the applications especially for those requiring compact portable setup [16,17], such as in vivo photoacoustic flow cytometry [18–21] and wearable PAM [22–24].

To simplify the manufacturing process and miniaturize the probe, here we present the design and construction of a 4 mm-outer diameter photoacoustic imaging probe prototype. A miniature TUT was fabricated using the LN wafer with the dimensions of 2 mm × 2 mm × 75 μm. Its center frequency was ~46.9 MHz with a bandwidth of 29.4%. A gradient-index (GRIN) lens was employed for beam shaping and as the backing layer of the TUT. The weight of the entire TUT was ~0.3 g. Moreover, the design allows the ease installation and replacement of single mode (SM) fibers for imaging using different laser wavelengths. The multi-functionality of the probe was validated by the experiments of fluid flow sensing and photoacoustic imaging, showing the promising potential for various biomedical application scenarios.

2. Materials and methods

2.1. Fabrication of TUT

A 10 mm × 10 mm LN wafer (Chenghan Optics, China) was selected and polished into 75 μm, and then coated with 150 nm-thick ITO on both surfaces. The wafer was cut into small pieces with the dimensions of 2 mm × 2 mm as the piezoelectric layer of the TUT. Figure 1a shows the schematic structure of the TUT. To fabricate the TUT, first of all, the LN wafer was positioned at the bottom of the brass housing using wax. The GRIN lens (GRIN2906, Thorlabs, USA) was adhered with the wafer by epoxy (301, Epoxy Technology Inc., USA). Secondly, the positive electrode of the wire was connected with the inner wall of the housing, while the negative one was adhered to the back side of the LN wafer using silver glue. Then, epoxy was applied to fix all the movable components. Finally, the silver glue was used to connect with the housing and the front side of the LN wafer after the epoxy was cured. Figure 1b shows the photo of TUT assembled with the SM fiber.

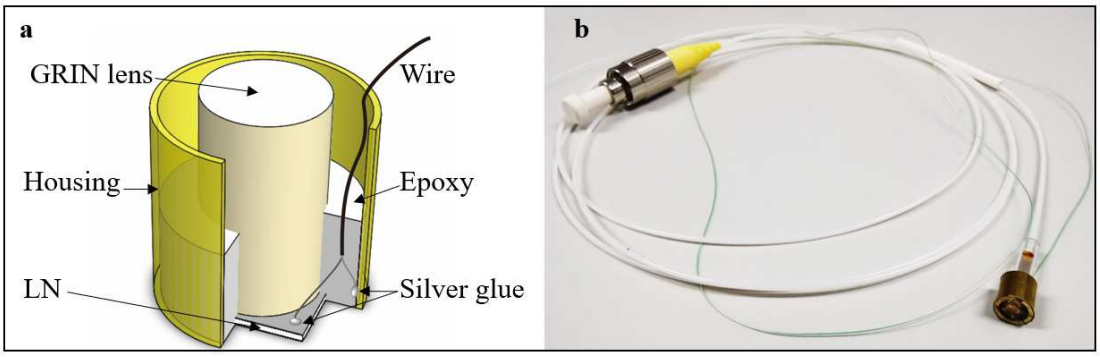

Figure 1. Schematic and photograph of a photoacoustic probe. (**a**) Structure of the probe; (**b**) Photograph of the miniature probe prototype.

2.2. Setup of system and photoacoustic probe

A pulsed Nd:YAG laser (Medical Technology (Shenzhen) Co., Ltd., China) with 532 nm wavelength was delivered through an iris and a beam expander (EX-532-2X-A, Sanke, China), then coupled into the SM fiber by an objective (PLAN 4X, Shangguang, China). The SM fiber (SMPF0106, Thorlabs, USA) with a pigtailed ferrule was applied for laser delivery. A ferrule sleeves (51-2800-1800, Thorlabs, USA) was used to align the GRIN lens and the fiber coaxially. The TUT was used to

Preprints (www.preprints.org) | NOT PEER-REVIEWED | Posted: 10 May 2023 doi:10.20944/preprints202305.0690.v1

detect photoacoustic signals from phantoms. The signal was sent to an ultrasound pulser/receiver (5073PR, Olympus, Japan) and then digitized with a DAQ board (ATS9371, Alazar Tech, Canada) in the computer. The schematics of system, probe and experiment setup are demonstrated in Figure 2.

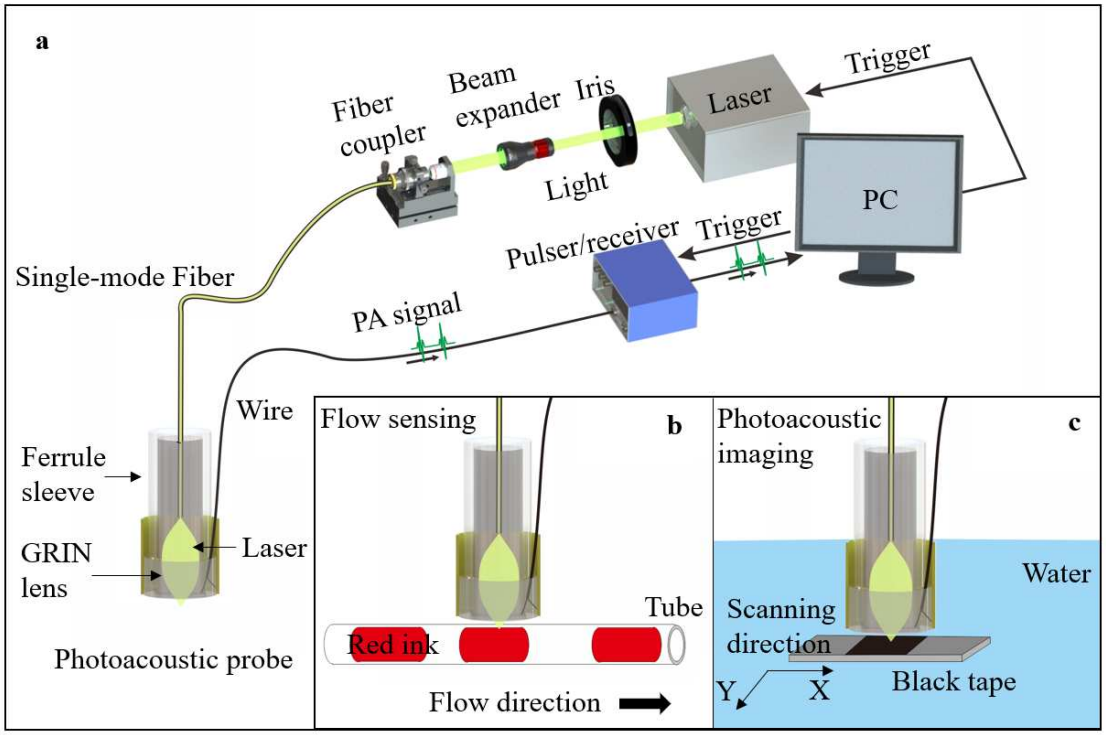

Figure 2. Schematics of system, probe and experiment setup. (**a**). 3D drawing of a system with the photoacoustic probe; (**b**). The schematic of flow sensing setup; (**c**). The schematic of photoacoustic imaging setup.

2.3. Performance test

To evaluate the acoustic performance of the TUT, a pulse-echo test was conducted. The ultrasound signals were received by the pulser/receiver and then displayed on a digital oscilloscope (DSOX2012A, Keysight, USA). An impedance analyzer (4294A, Agilent Tech., USA) was used for dielectric and electrical impedance measurements at room temperature.

To demonstrate the multi-functionality of probe, red ink and black tape were selected as targets in the setups of photoacoustic flow cytometry and photoacoustic microscopy as shown in Figure 2b,c. The red ink in a polyethylene (PE) tube was used for mimicking the blood in the vessel. The red ink was controlled by a pump (HL-2S, Shanghai Huxi, China), flowing at a rate of 3 cm/s.

To evaluate the imaging performance, the photoacoustic probe was fixed on a three-dimensional translation stage to scan the black tape in a water tank. Water was used as the medium of signal transmission.

3. Results

3.1. Performance of TUT

Figure 3a shows the measured pulse-echo response of TUT and its Fast Fourier Transform (FFT) spectra without gain. The results show that the measured center frequency of the transducer was 46.9 MHz with the -6 dB bandwidth of 29.4%. Figure 3b shows that the developed TUT exhibited an obvious resonance mode even the piezoelectric layer was loaded by the GRIN lens, in which the resonant frequency f_r was 41.3 MHz with the electrical impedance of 78 Ω. Compared to the desired

Preprints (www.preprints.org) | NOT PEER-REVIEWED | Posted: 10 May 2023 doi:10.20944/preprints202305.0690.v1

electrical impedance (50 Ω), the measured one was slightly higher that may be due to the imperfect electrical behavior of ITO electrodes.

With the anti-resonant frequency, f_a, of 47.2 MHz, the effective electromechanical coupling coefficient k_{eff} can be calculated by the following equation:

$$k_{eff} = \sqrt{1 - \frac{f_r^2}{f_a^2}}$$

The k_{eff} of the TUT was ~0.48, which is comparable to that of the reported TUT fabricated using LN as the piezoelectric material [11].

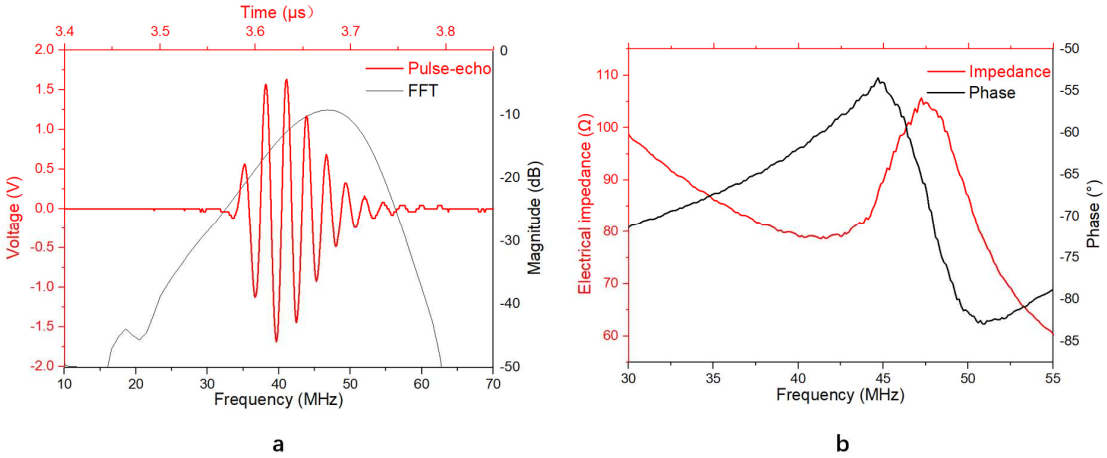

Figure 3. Performance of the TUT. (**a**) Pulse-echo results; (**b**) Impedance/phase frequency spectra.

3.2. Performance of photoacoustic probe

Figure 4 shows the sensing and imaging performance of the photoacoustic probe. Figure 4a,c are the photos of phantoms including the red ink in the PE tube and the black tape. Figure 4b presents the signals of flowing red ink, in which the yellow curve is the signal amplitude profile at the white dash line of B-scan photoacoustic signal. The result showed that the probe could distinguish the air bubbles from the flowing ink, being capable of telling if the fluid flow is continuous. Figure 4d shows the maximum amplitude projection (MAP) image of black tape, exhibiting the imaging capability of the probe.

Preprints (www.preprints.org) | NOT PEER-REVIEWED | Posted: 10 May 2023 doi:10.20944/preprints202305.0690.v1

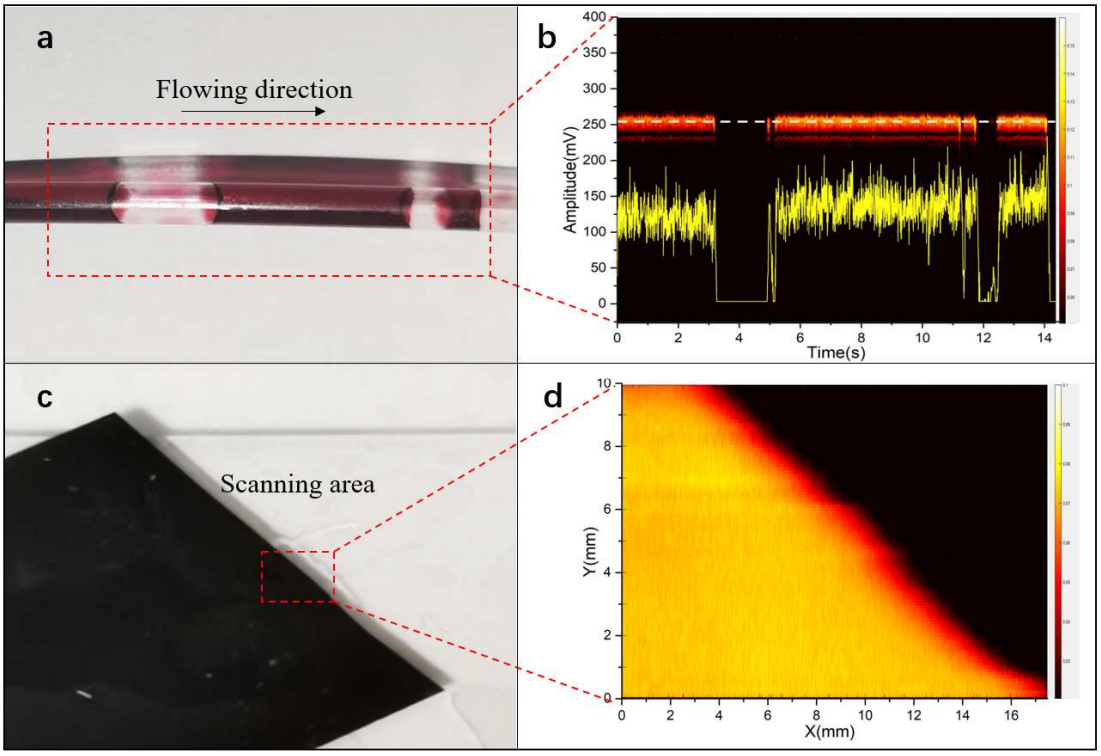

Figure 4. Photos and photoacoustic sensing/imaging results of phantoms. (**a**) Photo and (**b**) photoacoustic signals of red ink in tubing; (**c**) Photo and (**d**) photoacoustic image of a black tape.

4. Discussion and conclusion

The miniaturization and simplification of devices are conducive to clinical implementation. The reported transparent photoacoustic probes were mostly with centimeter-scale dimensions, limiting their application in the limited space. As the smaller LN wafer may only help to reduce the aperture size but likely degrade the transducer performance such as sensitivity, the issue can only be overcome via modifying the probe design and fabrication process.

The ITO thickness should be set in a reasonable range to balance the transparency and the electrical resistance. Different thicknesses of ITO were deposited and studied in terms of electrical properties. The thickness of 150 nm was optimized. To achieve the relatively low sheet resistance (~40 Ω ohm*cm), the sputtering process was operated at low power for a long duration.

To further shrink the probe size, we propose to combine the GRIN lens and the LN wafer as a whole. The GRIN lens is a key element for beam shaping. Epoxy was used as adhesion between the lens and LN wafer. The air bubbles in the epoxy could be removed by pressing the GRIN lens gently on the fragile wafer before curing.

There are two major types of optical fiber applied for laser delivery: the SM fiber offers a smaller spot while the multi-mode fiber offers higher laser energy. Both have the same packaging, so we chose the SM fiber with the pigtailed ferrule that was easy to align with the GRIN lens coaxially with the ferrule sleeve. With the proposed design, the fiber could be changed easily to meet various demands of applications.

The miniature probe was designed for multiple applications especially in the limited space. For example, an ideal flow cytometer is portable for placing on the skin to detect the blood and cells in the subcutaneous vessel. The probe should be small and light enough to be worn on the hand or arm. To evaluate the performance of flow sensing, the red ink and tube were used to mimic the blood and vessel. The signals of red ink and air bubbles could be easily identified (Figure 4b). While for the dynamic imaging, the probe could image the edge of black tape clearly as PAM. All the results suggested that the miniature probe was capable of performing different functions such as fluid flow sensing or photoacoustic imaging.

Though the results show the feasibility and potential of proposed photoacoustic probe, there are still rooms to further improve the performance. (1) As a miniature transducer, the bandwidth was too narrow though this is a common issue due to the limited option of transparent materials for matching and backing layers. To retain the transparency of the TUT, parylene was not deposited. The multi-matching layer scheme should be studied and applied on TUT to improve the bandwidth. (2) The GRIN lens could not absorb the ultrasound from the back of the LN wafer such that the echo signals and corresponding images would be adversely affected by ultrasound reflections. A longer GRIN lens may shift the unwanted reflections out of the ultrasound imaging range. (3) The mechanical scanning speed limits the potential of the probe especially for the application of PAM. Optical scanning could speed up the imaging, which should be studied in the future.

To summarize, a miniature photoacoustic probe based on a 4-mm diameter TUT was successfully developed. The GRIN lens was used as the backing layer of the TUT, effectively shrinking the probe size. The probe was tested and found to be with a high center frequency of 46.9 MHz and a -6 dB bandwidth of 29.4%. Experiments were further conducted on the mimicking phantom and black tape to show the potentials in the fluid flow sensing and imaging applications, respectively.

Funding: This work was supported by grants from the National Natural Science Foundation of China (62005306, 82027803, 61975226); the CAS Key Laboratory of Health Informatics (2011DP173015); the Guangdong Provincial Key Laboratory of Biomedical Optical Imaging Technology (2020B121201010); Hong Kong Research Impact Fund (R5029-19), Hong Kong Research Grants Council (15220920); the Shenzhen Science and Technology Innovation Committee (ZDSY20130401165820357, JCYJ20200109114610201). Shenzhen Engineering Laboratory for Diagnosis & Treatment key technologies of interventional surgical robots (XMHT20220104009).

Institutional Review Board Statement: Not applicable.

Data Availability Statement: Data underlying the results presented in this paper are not publicly available at this time but may be obtained from the authors upon reasonable request.

Conflicts of Interest: The authors declare that there are no conflicts of interest.

References

1. Attia ABE, Balasundaram G, Moothanchery M, Dinish US, Bi R, Ntziachristos V, Olivo M. A review of clinical photoacoustic imaging: Current and future trends. Photoacoustics 2019, **16:** 100144.
2. Jeon S, Kim J, Lee D, Baik JW, Kim C. Review on practical photoacoustic microscopy. Photoacoustics 2019, **15:** 100141.
3. Wang LV, Yao J. A practical guide to photoacoustic tomography in the life sciences. Nat Methods 2016, **13**(8)**:** 627-638.
4. Liu W, Yao J. Photoacoustic microscopy: principles and biomedical applications. Biomed Eng Lett 2018, **8**(2)**:** 203-213.
5. Maslov K, Stoica G, Wang LV. In vivo dark-field reflection-mode photoacoustic microscopy. Opt Lett 2005, **30**(6)**:** 625-627.
6. Maslov K, Zhang HF, Hu S, Wang LV. Optical-resolution confocal photoacoustic microscopy. Photons Plus Ultrasound: Imaging and Sensing 2008: The Ninth Conference on Biomedical Thermoacoustics, Optoacoustics, and Acousto-optics; 2008: SPIE; 2008. p. 449-455.
7. Hu S, Maslov K, Wang LV. Second-generation optical-resolution photoacoustic microscopy with improved sensitivity and speed. Opt Lett 2011, **36**(7)**:** 1134-1136.
8. Qin W, Jin T, Guo H, Xi L. Large-field-of-view optical resolution photoacoustic microscopy. Opt Express 2018, **26**(4)**:** 4271-4278.
9. Wang H, Yang X, Liu Y, Jiang B, Luo Q. Reflection-mode optical-resolution photoacoustic microscopy based on a reflective objective. Opt Express 2013, **21**(20)**:** 24210-24218.
10. Dangi A, Agrawal S, Kothapalli SR. Lithium niobate-based transparent ultrasound transducers for photoacoustic imaging. Opt Lett 2019, **44**(21)**:** 5326-5329.
11. Chen R, He Y, Shi J, Yung C, Hwang J, Wang LV, Zhou Q. Transparent High-Frequency Ultrasonic Transducer for Photoacoustic Microscopy Application. IEEE Trans Ultrason Ferroelectr Freq Control 2020, **67**(9)**:** 1848-1853.
12. Chen H, Mirg S, Osman M, Agrawal S, Cai J, Biskowitz R, Minotto J, Kothapalli SR. A High Sensitivity Transparent Ultrasound Transducer based on PMN-PT for Ultrasound and Photoacoustic Imaging. IEEE Sens Lett 2021, **5**(11)**:** 1-4.
13. Brodie GW, Qiu Y, Cochran S, Spalding GC, MacDonald MP. Optically transparent piezoelectric transducer for ultrasonic particle manipulation. IEEE Trans Ultrason Ferroelectr Freq Control 2014, **61**(3)**:** 389-391.

14. Peng HB, Cheng ZW, Zeng L, Ji XR. Photoacoustic microscopy based on transparent piezoelectric ultrasound transducers. J Innov Opt Heal Sci 2023.
15. Park J, Park B, Kim TY, Jung S, Choi WJ, Ahn J, Yoon DH, Kim J, Jeon S, Lee D, Yong U, Jang J, Kim WJ, Kim HK, Jeong U, Kim HH, Kim C. Quadruple ultrasound, photoacoustic, optical coherence, and fluorescence fusion imaging with a transparent ultrasound transducer. Proceedings of the National Academy of Sciences of the United States of America 2021, **118**(11).
16. Tang J, Coleman JE, Dai X, Jiang H. Wearable 3-D Photoacoustic Tomography for Functional Brain Imaging in Behaving Rats. Sci Rep 2016, **6:** 25470.
17. Hariri A, Lemaster J, Wang J, Jeevarathinam AS, Chao DL, Jokerst JV. The characterization of an economic and portable LED-based photoacoustic imaging system to facilitate molecular imaging. Photoacoustics 2018, **9:** 10-20.
18. Edgar RH, Samson AP, Kocsis T, Viator JA. Photoacoustic Flow Cytometry Using Functionalized Microspheres for Selective Detection of Bacteria. Micromachines (Basel) 2023, **14**(3)**:** 573.
19. Suo Y, Gu Z, Wei X. Advances of In Vivo Flow Cytometry on Cancer Studies. Cytometry A 2020, **97**(1)**:** 15-23.
20. Song Z, Fu Y, Qu J, Liu Q, Wei X. Application of convolutional neural network in signal classification for in vivo photoacoustic flow cytometry. Optics in Health Care and Biomedical Optics X; 2020: SPIE; 2020. p. 363-369.
21. Liu Q, Zhou Q, Fu Y, Zhu X, Tao L, Wei X. Label-free counting of circulating melanoma cells in deep vessels with photoacoustic flow cytometry. Biophotonics and Immune Responses XV; 2020: SPIE; 2020. p. 52-57.
22. Chen Q, Xie H, Xi L. Wearable optical resolution photoacoustic microscopy. J Biophotonics 2019, **12**(8)**:** e201900066.
23. Dangi A, Agrawal S, Datta GR, Srinivasan V, Kothapalli SR. Towards a Low-Cost and Portable Photoacoustic Microscope for Point-of-Care and Wearable Applications. IEEE Sens J 2020, **20**(13)**:** 6881-6888.
24. Chen Q, Jin T, Qi W, Xi L. Dual-model wearable photoacoustic microscopy and electroencephalograph: study of neurovascular coupling in anesthetized and freely moving rats. Biomed Opt Express 2021, **12**(10)**:** 6614-6628.